Experimental investigation into the initiation of head check damage using v-track

Ren, Fang; Yang, Zhen; Hajizad, Omid; Moraal, Jan; Li, Zili

Publication date
2022

Document Version
Final published version

Published in
CM 2022 - 12th International Conference on Contact Mechanics and Wear of Rail/Wheel Systems, Conference Proceedings

12th International Conference on Contact Mechanics and Wear of Rail/Wheel Systems (CM2022), Melbourne, Australia, 4-7 September 2022

EXPERIMENTAL INVESTIGATION INTO THE INITIATION OF HEAD CHECK DAMAGE USING V-TRACK

Fang Ren*, Zhen Yang, Omid Hajizad, Jan Moraal, Zili Li

Delft University of Technology, Stevinweg 1, 2628 CN, Delft, the Netherlands

* E-mail: f.ren-1@tudelft.nl

Abstract:
Rolling contact fatigue (RCF) has been a persistent type of damage in rails. To guarantee the safety of railway operation and reduce the maintenance cost, various tests have been conducted to study the RCF damage. In this research, a state-of-the-art downscaled V-Track test rig at TU Delft was used to investigate the initiation of the head check (HC), a typical type of RCF damage. The V-Track test was designed to simulate the wheel-rail contact conditions with the stress state and spin creepage as similar as that in the field. The test rig ran up to 60,000 load cycles, after which significant surface damage in the form of surface irregularity and cracks was observed in two different zones on the rails. The test results demonstrated that the V-Track is capable of maintaining steady-state loading conditions after a high number of load cycles. Using the same loading condition, a contact stress analysis was subsequently performed to identify the surface stress distribution and predict the pattern of plastic flow inside the contact patch. The plastic flow prediction was then confirmed by a microscopic analysis of the samples cut from the V-Track rails. Furthermore, the microscopic analysis indicated an opposite orientation of the plastic flow in the zone outside contact patch, which will be investigated in further studies.

Keywords: Rolling contact fatigue, head check, V-Track, microscopic analysis, contact patch, plastic flow.

1. Introduction

Head check (HC) as a type of rolling contact fatigue (RCF) has been a persistent problem for the modern railways. HC damage appears on the rail surface as clusters of inclined, regularly and closely distanced cracks. While grinding has been a viable solution to limit the growth of HC damage, the cost effectiveness remains a challenge as for the timing and extent of the material removal or even rail replacement. Untimely and inadequate dealing with the HC damages may cause substantial economical consequence and even fatal accidents [1]. To effectively overcome this, an accurate prediction of the rail fatigue in terms of HC crack initiation and propagation [2] is desirable.

During curving, the leading wheelset of a bogie experiences high lateral creep forces due to the large angle of attack. The contact shifts from rail top towards the gauge side. The rail shoulder or gauge corner comes into contact with the wheel where the profile has large conicity and thus large geometrical spin takes place. The large surface shear stress induced by the geometrical spin can be a main cause of head check initiation [3].

When the surface shear stress exceeds the plastic shakedown limit, ratcheting occurs under the cyclic loading [4]. With the accumulated load cycles, crack initiation can be traced in the layer of plastic deformation following the direction of the plastic flow [5]. The further growth of the cracks is then driven by the cyclic shear stress and can be exacerbated by the fluid entrapped in the cracks [6, 7]. With the crack propagation extended, horizontal and vertical branching occurs and eventually leads to shelling or forced fracture [8].

To investigate the RCF damage mechanism, various tests have been performed to generate the RCF. Twin-disc tests are widely used to simulate the contacts between wheel and rail with clusters of RCF cracks generated [2, 5, 9~11]. With controlled creepage and loading, Tyfour et al [2] proposed an empirical model to predict the initiation and propagation of RCF cracks. Kapoor et al [9] validated their numerical model in predicting rail surface ratcheting related to RCF crack initiation. Hiensch and Burgelman [10] developed an RCF damage function for the R220 rail steel grade incorporating the influence of wear. The twin-disc tests have their advantage of the ease of setting up and controlling the test parameters. By adjusting the rotation and alignment of the discs, the longitudinal [11] and lateral creepage [12] can be controlled and monitored during the tests.

RCF (HC in particular) cracks have also been successfully generated on the Voestalpine test rig [13, 14, 15] , which consists of a full-scale wheel and a 1.5-m-long straight rail in reciprocating motion. For this test rig, the wheel-rail contact loads are generated by hydraulic cylinders exerting both vertical and horizontal loads on the test track in contact with the wheel. The test rig can generate the realistic contact conditions with its full-scale contact radii per the exerted loads with the maximum running speed of 0.5 m/s [14].

Nonetheless, the aforementioned twin-disc test rigs cannot properly represent the hardness of a head-hardened rail due to the way the discs/rollers are made [16, 17]. As to the full-scale test rigs, their efficiency is limited by the operational speed, the accurate control of

***Figure 1**: The V-Track test rig*

the wheel-rail contact conditions, and potentially high costs . Furthermore, it has been reported that the head-hardened rail is more RCF resistant [14] and new rail steel materials such as bainitic steel has better mechanical properties [18]. Since large number of load cycles is generally needed for fatigue tests, a test rig capable of testing multiple rail material simultaneously is preferred.

In this research, the test rig V-Track (Figure 1) [19] is used to investigate the HC crack initiation and propagation under controlled and monitored loading conditions. Compared to the twin-disc tests, the scaled rail extracted from the original hardened rail head can accurately represent the hardness distribution in the rail head. The contact radii can be flexibly controlled by using bespoke profiles of rail and wheel. Moreover, multiple rail steel grades can be incorporated in one setup and tested simultaneously, which is desirable for the study of HC initiation and propagation in different rail steel materials.

2. Methodology

2.1. V-Track

The V-Track test rig was developed in-house by the Section of Railway Engineering at TU Delft. This scaled test rig with a ring of circular rail of 2m radius can simulate various phenomena induced by wheel-track interaction such as rail corrugation, track vibration, RCF, etc. [19]. Depending on the test setups, the rail ring can be divided into multiple sections, each with a different steel grade. The rails are then clamped to 100 scaled sleepers underneath. Four wheels loaded with compressed springs simulating vertical force from the primary suspension can run continuously at a maximum speed of 40 km/h. Each wheel is equipped with multiple force and vibration sensors to instantaneously record the test data including the wheel-rail contact force in three directions [20].

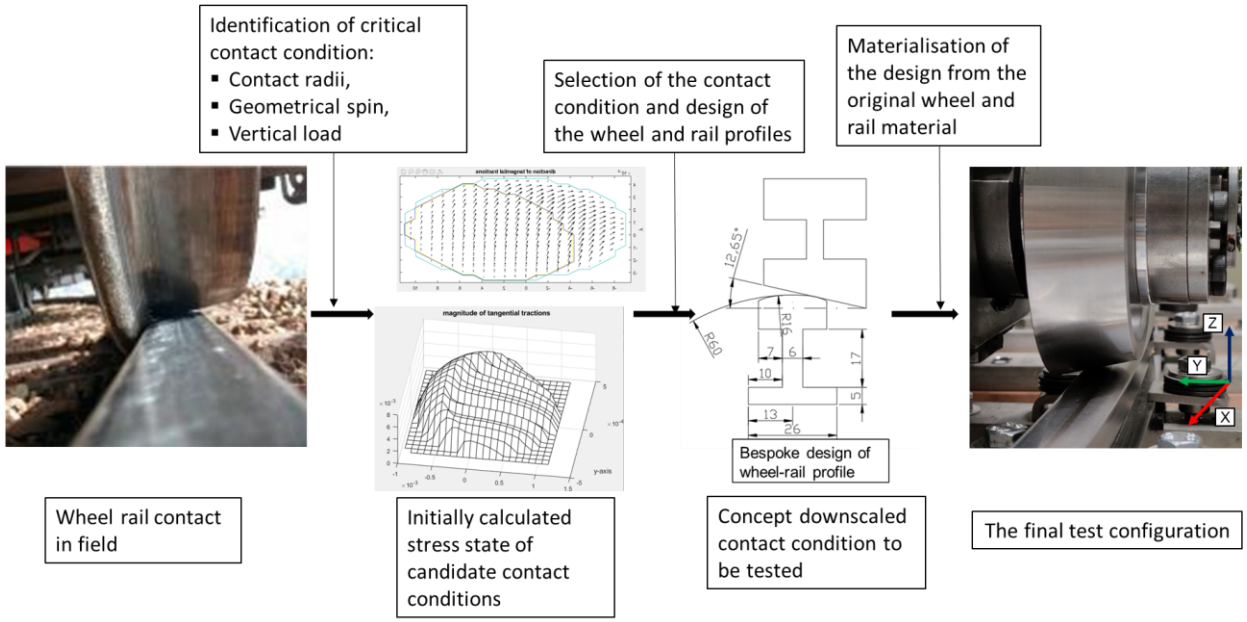

***Figure 2** The test design process*

2.2. Test design

The contact and loading conditions, including contact geometry, the coefficients of friction, contact loads and rail and wheel materials, were controlled to replicate the contact stress state under geometrical spin creepage [13]. The geometrical spin is realised by matching the conicity of wheel and the contact radius of the scaled rail profile. In addition, a torque can be applied to the wheel axle to simulate positive longitudinal force experienced by a driving wheel. The design process of the test is illustrated in Figure 2.

Four steel grades are tested simultaneously on the test rig with each rail section made of one steel grade spanning over a range of 25 sleepers. The four steel grades of rail material selected for the tests are two naturally hard pearlitic steel grades, R220 (sleeper No. 26-50) and R260MN (sleeper No. 51-75), one head-hardened pearlitic steel, MHH (sleeper No. 76-100), and one bainitic steel, B320 (Sleeper No 1-25). R260MN and MHH are widely used in the Dutch railway. The softest rail material R220 is selected as a reference to assess the influence of wear on the HC crack propagation. B320 is tested to extend the knowledge of head check generation to the bainitic steel rail. This paper will focus on the results from R260MN at the current stage.

2.3. Load case

The load case was designed to simulate the rail-wheel contact during curving in the real life. An average of 3500N of vertical load was used per wheel on V-Track. This can induce a Hertzian contact pressure higher than 2 GPa calculated based on the contact radii of the rail and wheel, which was determined from the HC tests on the Voestalpine test rig [13]. With the designed conicity of 12.65 degrees of the wheel profile, the geometrical spin creepage would also generate a lateral force component at contact. Furthermore, a positive torque was applied to simulate the condition of a driving wheel. The torque can generate an average traction coefficient of 0.15. The total adhesion coefficient, considering both longitudinal and the lateral forces, was around 0.20 during the test.

2.4. Contact stress

The initial contact stress state was calculated with CONTACT [21]. The orientation of the surface shear stress calculated with linear elasticity gives an indication of the possible plastic flow direction in the rail. The plastic flow can be observed from the microscopic analysis of the samples cut from the testing rails, which was then compared with the results predicated by using CONTACT.

2.5. Microscopic analysis

Microscopic analysis was performed to investigate the plastic deformation and flow pattern. Samples were cut from the test rail section on the V-Track. Two types of samples were cut, polished, and etched: the longitudinal and transverse samples, as shown in Figure 3. The longitudinal sample was cut along the running direction of the wheel and into the depth of the rail. Since the cracks were small on the downscaled rails compared to those in the field, the longitudinal sample was initially cut at the edge of the suspected surface damage and then ground by steps to the crack locations of interest. At each grinding step, the light optical microscope (LOM) observation was performed to investigate the plastic deformation along the depth in the longitudinal direction of the samples. The transverse sample was cut perpendicularly to the running direction and observed

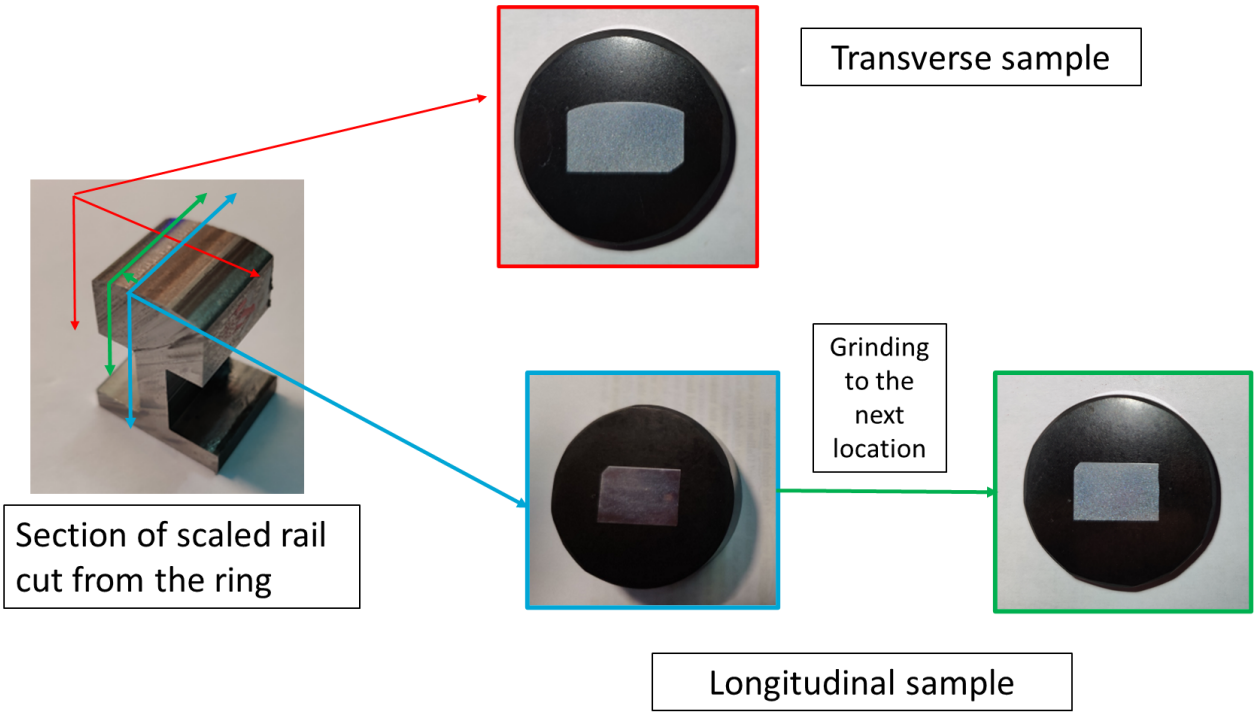

Figure 3 *Illustration of the sample cutting/grinding strategy for transverse and longitudinal samples. The red, blue and green arrows indicate the cutting directions for transverse and longitudinal samples and the grinding direction for longitudinal samples*

only once to trace the patterns in plastically deformed region along the depth of the material. These two types of samples would provide good overview of the plastic deformation of rail head material, which is critical for the further investigation of HC damage.

3. Results

3.1. Load repeatability

Figure 4 shows the repeatability of wheel-rail contact forces measured in the V-Track. The tests were terminated after 60,000 load cycles with substantial cracks observed. The measured longitudinal and vertical forces show the resemblance in pattern and amplitudes throughout the load cycles as per Figure 4 (a) and (c). This indicates that the V-Track can provide steady-state loading condition for the RCF tests with a large number of load cycles. There is, however, some difference in the lateral forces among the different load cycles as shown in Figure 4 (c). The difference was caused by the slight change in contact geometry due to the wear and deformation in rail and wheel resulting in larger lateral loads at higher load cycles.

3.2. Contact stress analysis

The contact stress was calculated at each sample cutting locations. The results at sleeper No. 72 are presented

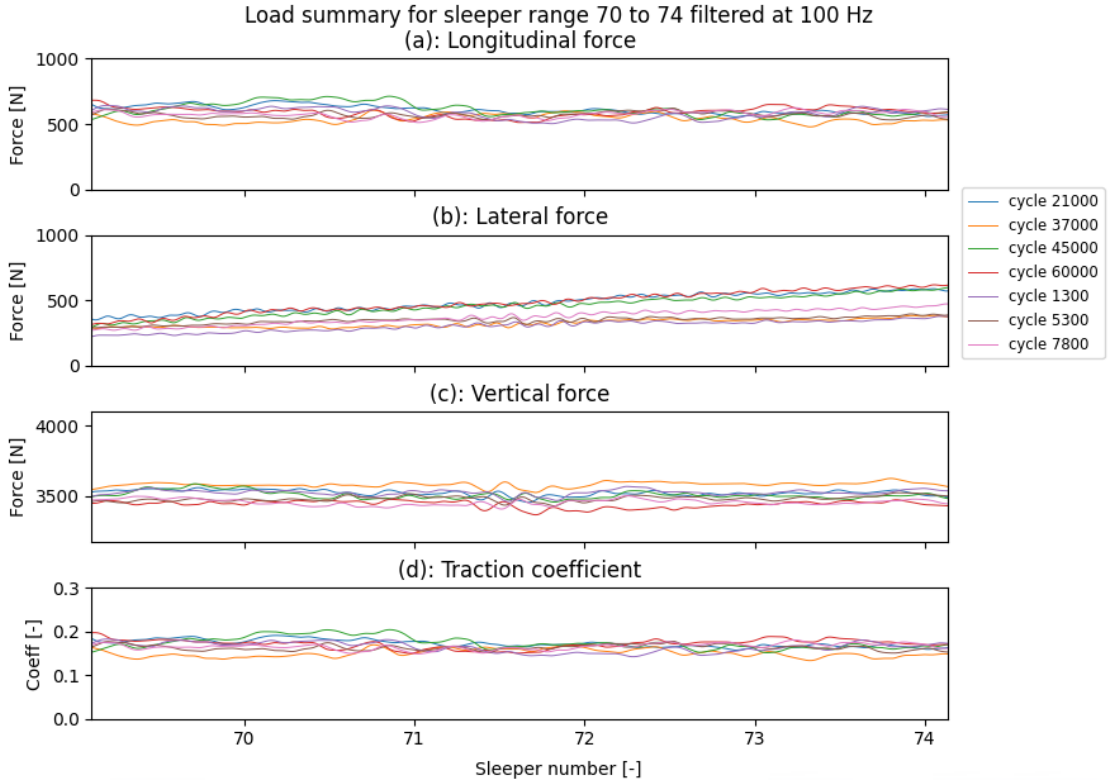

Figure 4 *The comparison of the contact forces on the wheel measured in the V-Track test rig in different load cycles at sleeper NO. 69 to 74: (a) the longitudinal forces (b) the lateral forces (c) the vertical forces (d) traction coefficient*

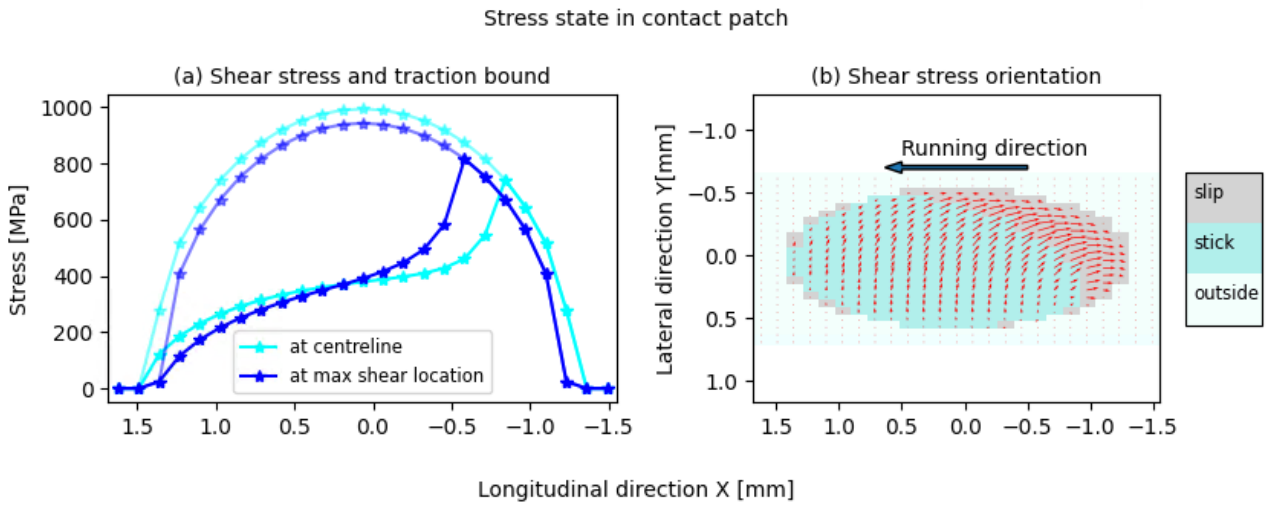

Figure 5 *The contact stress state calculated with CONTACT, (a) the comparison of the shear stress amplitude and the traction bound, (b) the orientation pattern of the surface shear stress inside the contact patch*

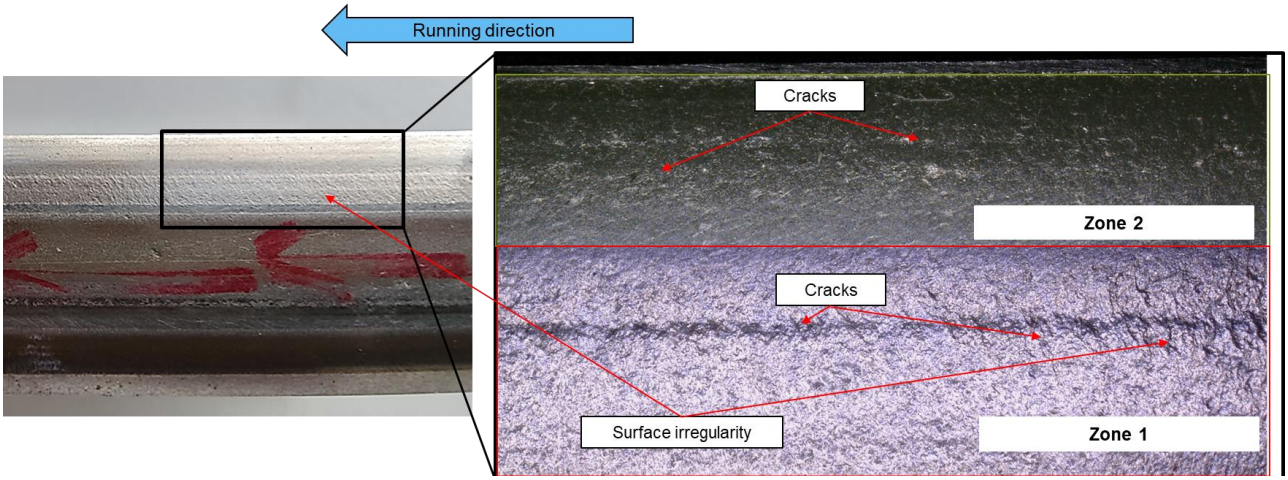

Figure 6 *Surface damage recorded at load cycle 60,000 within and out of the running band.*

here. The rail steel grade at this location is R260MN, which showed the most significant development of the surface damage in the form of surface irregularities and cracks during the test. The load shown in Figure 4 is used to determine the initial contact condition. Since the CONTACT program does not consider plasticity [21], the pattern of shear stress orientation is of more interest than the magnitude of the stresses.

The surface stress state in the contact patch is shown in Figure 5. Because a driving wheel was simulated, the surface shear stress in the longitudinal direction is opposite to the running direction. Moreover, the orientations of the lateral shear components are general towards the minus Y axis or to the right when looking in the running direction. In addition, the shear stress in the contact patch shows a rotational pattern due to the geometrical spin creepage. This pattern displays an uneven distribution of shear stress in the contact patch, i.e. the high shear stress components are located on the right side of the contact patch following the running direction.

Since shear stress plays a crucial role in the yield of the rail steel [4, 9], the orientation of the surface shear stress can be used to forecast the direction of plastic flow in the contact patch. In the longitudinal direction, the plastic deformation should hence flow to the opposite of the running direction. In the lateral direction, the plastic deformation should be more concentrated to the right part of the contact patch and orientate towards right with respect to the running direction. This will be compared and verified in Section 3.4.

3.3. Surface damage

Surface damage appeared as surface irregularities and cracks after about 10,000 load cycles on the R260MN rail. When the test was terminated at 60,000 cycles, significant surface damage was captured in two different zones on the rail top, as indicated in Figure 6. In Zone 1, clusters of inclined cracks were seen orientated towards the running direction. High occurrence of surface irregularity was also be observed in this zone. Zone 2 was darker and exhibited much less surface irregularity possibly due to the repetitive wheel passages. Clusters of cracks were identified in this zone but with less obvious orientation. Besides the appearance of the surface damage, difference in the plastic flow can also be observed in the two zones, which will be further elaborated in Section 3.4.

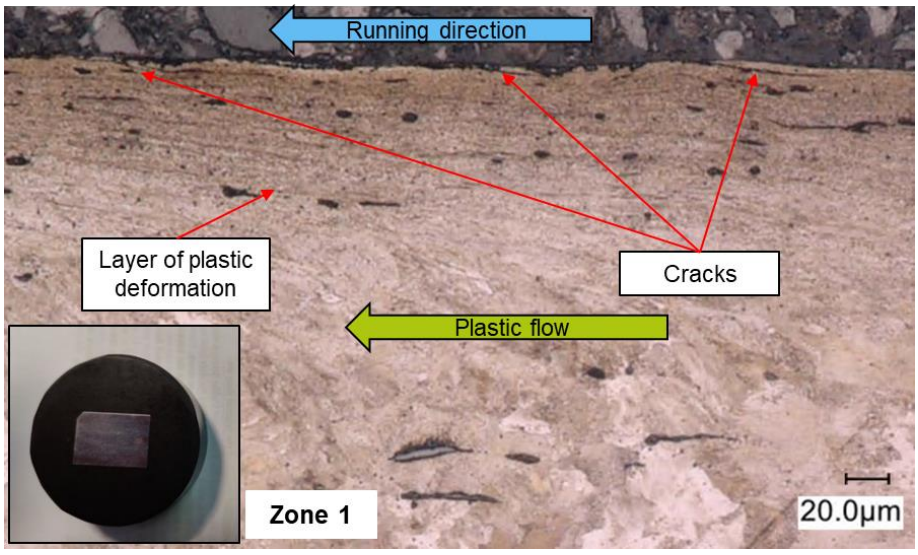

Figure 7 *LOM image from a longitudinal sample at the centreline of the Zone 1*

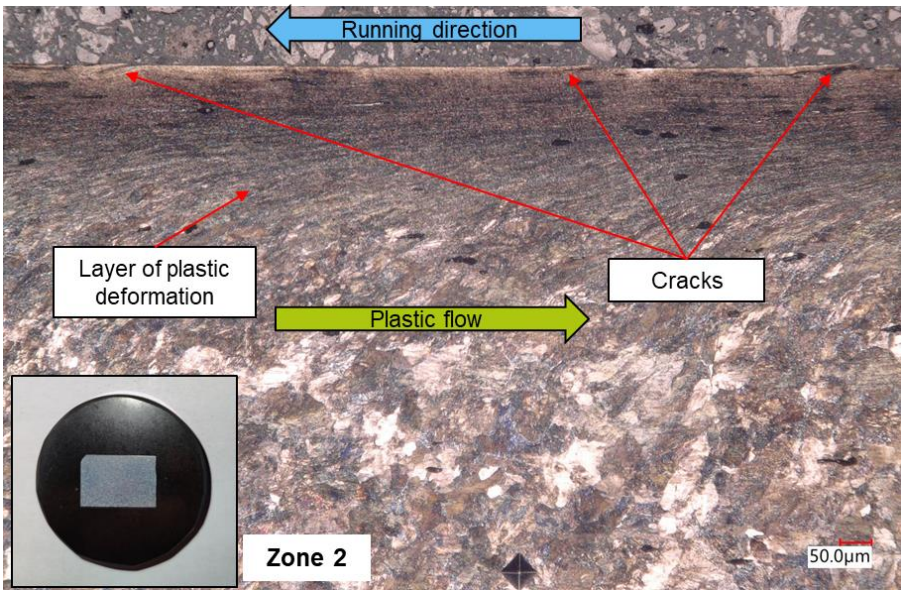

Figure 8 *LOM image from a longitudinal sample at the centreline of Zone 2*

3.4. Microscopic analysis

The plastic flow from a longitudinal rail sample that was ground to the centreline of Zone 1 is shown in Figure 7. It is indicated that the plastic flow orientated in the same direction as the running wheel. In the plastic deformed layer, surface cracks were visible and propagated along the orientation of the plastic deformation. Furthermore, surface irregularity can be observed at the top edge of the sample corresponding to the pattern seen in Zone 1 as per Figure 6. It is worth noting that the plastic flow direction in Zone 1 was found opposite to what was predicted within the contact patch in Section 3.2.

Contrary to the results observed in Zone 1, the sample from Zone 2 exhibited a plastic flow opposite to the running direction as per Figure 8. Cracks opposite to the running direction can be observed in between the plastically deformed laminar. The orientation of plastic deformation agrees with the results predicted for the contact patch.

The microscopic results of the transverse sample demonstrate good agreement with the contact solution in Section 3.2. As shown in Figure 9, the deeper plastic deformation can be observed on the right side of the running band following the running direction, which corresponds to the high shear stress region shown in Figure 5. The plastic flow shown in Figure 10 had the same orientation with the lateral component of the shear stress in the contact patch. Cracks were also clearly visible following the plastic flow in the transvers sample.

The microscopic analysis results showed that in Zone 2, the plastic flow orientation agrees well with the shear stress pattern. This demonstrates that the orientation of the shear stress within the contact patch determines the

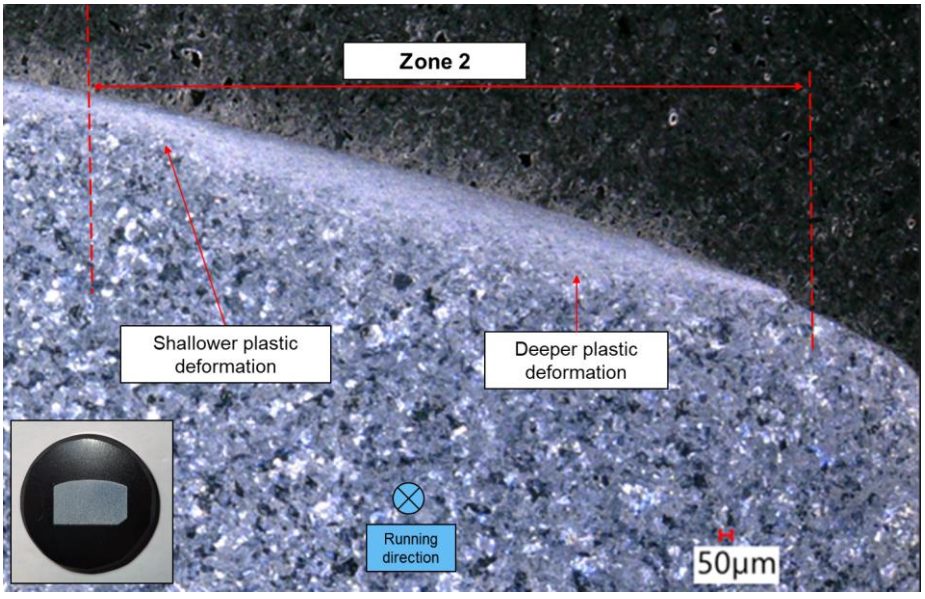

Figure 9 *Plastic deformation compared in the transverse sample (the running direction points into the figure)*

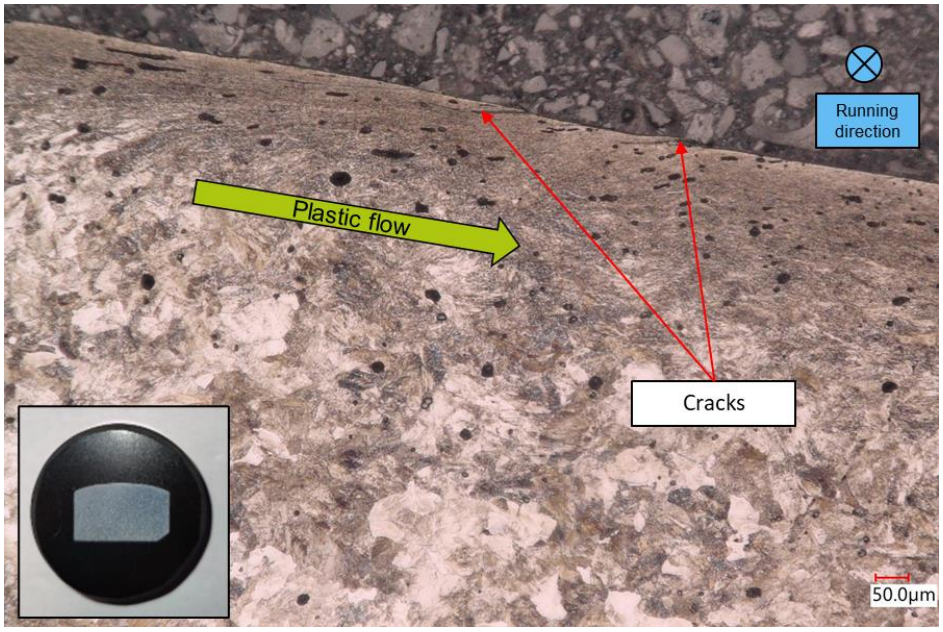

Figure 10 *The plastic flow from the transverse sample (the running direction points into the figure)*

direction of plastic flow generated in the running band. The cracks found in this zone are thus expected to develop into HC cracks. In Zone 1, the plastic flow shows an opposite trend. A possible explanation could be that the residual stress was accumulated with wheel passages and generated a plastic flow in the running direction outside the contact patch.

4. Conclusion

This paper shows that the V-Track test rig is able to generate RCF-induced surface damage in the tested rail surface under controlled contact conditions. The wheel-rail contact forces measured by the V-Track show good repeatability of the loading conditions for a large number of load cycles. Based on the tested loading conditions, contact stress analysis was used to predict the orientation of plastic flow within the running band according to the shear stress pattern in the contact patch. Subsequently, the plastic flow in the rail was assessed from a microscopic analysis which confirms the correlation between the surface shear stress and plastic flow patterns in both the longitudinal and lateral directions. Moreover, the microscopic analysis also shows an opposition pattern of the plastic flow outside the contact patch. This phenomenon will be investigated further.

References

[1] S. L. Grassie, "Rolling contact fatigue on the British railway system: treatment," *Wear,* vol. 258, pp. 1310-1318, 3 2005.

[2] W. R. Tyfour, J. H. Beynon and A. Kapoor, "Deterioration of rolling contact fatigue life of pearlitic rail steel due to dry-wet rolling-sliding line contact," *Wear,* vol. 197, pp. 255-265, 9 1996.

[3] R. Dollevoet, Z. Li and O. Arias-Cuevas, "A Method for the Prediction of Head Checking Initiation Location and Orientation under Operational Loading Conditions," *Proceedings of the Institution of Mechanical Engineers, Part F: Journal of Rail and Rapid Transit,* vol. 224, pp. 369-374, 7 2010.

[4] A. F. Bower and K. L. Johnson, "The influence of strain hardening on cumulative plastic deformation in rolling and sliding line contact," *Journal of the Mechanics and Physics of Solids,* vol. 37, pp. 471-493, 1 1989.

[5] G. Donzella, A. Mazzù and C. Petrogalli, "Competition between wear and rolling contact fatigue at the wheel-rail interface: Some experimental evidence on rail steel," *Proceedings of the Institution of Mechanical Engineers, Part F: Journal of Rail and Rapid Transit,* vol. 223, pp. 31-44, 1 2009.

[6] A. F. Bower, "The Influence of Crack Face Friction and Trapped Fluid on Surface Initiated Rolling Contact Fatigue Cracks," *Journal of Tribology,* vol. 110, pp. 704-711, 10 1988.

[7] D. I. Fletcher, F. J. Franklin and A. Kapoor, "Rail surface fatigue and wear," R. Lewis and U. Olofsson, Eds., Elsevier, 2009, pp. 280-310.

[8] R. Heyder and M. Brehmer, "Empirical studies of head check propagation on the DB network," *Wear,* vol. 314, pp. 36-43, 6 2014.

[9] A. Kapoor, J. H. Beynon, D. I. Fletcher and M. Loo-Morrey, "Computer simulation of strain accumulation and hardening for pearlitic rail steel undergoing repeated contact," *The Journal of Strain Analysis for Engineering Design,* vol. 39, p. 383–396, 5 2004.

[10] M. Hiensch and N. Burgelman, "Rolling contact fatigue: Damage function development from two-disc test data," *Wear,* Vols. 430-431, pp. 376-382, 7 2019.

[11] D. I. Fletcher and S. Lewis, "Creep curve

measurement to support wear and adhesion modelling, using a continuously variable creep twin disc machine," *Wear*, Vols. 298-299, pp. 57-65, 2 2013.

[12] A. D. Monk-Steel, D. J. Thompson, F. G. Beer and M. H. A. Janssens, "An investigation into the influence of longitudinal creepage on railway squeal noise due to lateral creepage," *Journal of Sound and Vibration*, vol. 293, pp. 766-776, 6 2006.

[13] R. P. B. J. Dollevoet, Design of an Anti Head Check profile based on stress relief, PhD thesis, 2010.

[14] R. Stock and R. Pippan, "RCF and wear in theory and practice—The influence of rail grade on wear and RCF," *Wear*, vol. 271, p. 125–133, 5 2011.

[15] D. T. Eadie, D. Elvidge, K. Oldknow, R. Stock, P. Pointner, J. Kalousek and P. Klauser, "The effects of top of rail friction modifier on wear and rolling contact fatigue: Full-scale rail-wheel test rig evaluation, analysis and modelling," *Wear*, vol. 265, pp. 1222-1230, 10 2008.

[16] A. C. Athukorala, D. V. D. Pellegrin and K. I. Kourousis, "Characterisation of head-hardened rail steel in terms of cyclic plasticity response and microstructure for improved material modelling," *Wear*, Vols. 366-367, pp. 416-424, 11 2016.

[17] Y. Zhou, S. Wang, T. Wang, Y. Xu and Z. Li, "Field and laboratory investigation of the relationship between rail head check and wear in a heavy-haul railway," *Wear*, vol. 315, pp. 68-77, 7 2014.

[18] O. Hajizad, A. Kumar, Z. Li, R. H. Petrov, J. Sietsma and R. Dollevoet, "Influence of microstructure on mechanical properties of bainitic steels in railway applications," *Metals*, vol. 9, p. 778, 7 2019.

[19] M. Naeimi, Z. Li, R. H. Petrov, J. Sietsma and R. Dollevoet, "Development of a New Downscale Setup for Wheel-Rail Contact Experiments under Impact Loading Conditions," vol. 42, pp. 1-17, 10 2017.

[20] P. Zhang, J. Moraal and Z. Li, "Design, calibration and validation of a wheel-rail contact force measurement system in V-Track," *Measurement*, vol. 175, p. 109105, 4 2021.

[21] J. J. Kalker, Three-Dimensional Elastic Bodies in Rolling Contact, Springer Netherlands, 1990.